Physica Medica 57 (2019) 72–79

Contents lists available at ScienceDirect

Physica Medica

journal homepage: www.elsevier.com/locate/ejmp

Original paper

Dose distribution verification in high-dose-rate brachytherapy using a highly sensitive normoxic *N*-vinylpyrrolidone polymer gel dosimeter

Yusuke Watanabe[a,*], Shinya Mizukami[a], Kou Eguchi[b], Takuya Maeyama[c], Shin-ichiro Hayashi[d], Hiroshi Muraishi[a,b], Tsuyoshi Terazaki[e], Tsutomu Gomi[a,b]

[a] School of Allied Health Sciences, Kitasato University, Sagamihara, Kanagawa, Japan
[b] Kitasato University Graduate School of Medical Sciences, Sagamihara, Kanagawa, Japan
[c] School of Science, Kitasato University, Sagamihara, Kanagawa, Japan
[d] Faculty of Health Sciences, Hiroshima International University, Higashi-Hiroshima, Hiroshima, Japan
[e] Department of Radiology, Kitasato University Hospital, Sagamihara, Kanagawa, Japan

ARTICLE INFO

Keywords:
High-dose-rate brachytherapy
Iridium-192
Polymer gel dosimeter
MRI

ABSTRACT

Rapid technological advances in high-dose-rate brachytherapy have led to a requirement for greater accuracy in treatment planning system calculations and in the verification of dose distributions. In high-dose-rate brachytherapy, it is important to measure the dose distribution in the low-dose region at a position away from the source in addition to the high-dose range in the proximity of the source. The aim of this study was to investigate the accuracy of a treatment plan designed for prostate cancer in the low-dose range using a normoxic *N*-vinylpyrrolidone-based polymer gel (VIPET gel) dosimeter containing inorganic salt as a sensitizer (iVIPET). The dose response was evaluated on the basis of the transverse relaxation rate (R_2) measured by magnetic resonance scanning. In the verification of the treatment plan, gamma analysis showed that the dose distributions obtained from the polymer gel dosimeter were in good agreement with those calculated by the treatment planning system. The gamma passing rate according to the 2%/2 mm criterion was 97.9%. The iVIPET gel dosimeter provided better accuracy for low doses than the normal VIPET gel dosimeter, demonstrating the potential to be a useful tool for quality assurance of the dose distribution delivered by high-dose-rate brachytherapy.

1. Introduction

In high-dose-rate (HDR) brachytherapy, a radioisotope source is transported directly to a precise location within or near to a tumour using a remote afterloading system. Iridium-192 (Ir-192) is commonly used as the radioisotope for the source because of its availability and high radioactivity. The treatment planning system (TPS) optimises the dose distributions, establishes safe positions for the source and calculates the appropriate dwell time. Using HDR brachytherapy, a high dose can be delivered to a tumour while the surrounding normal tissue is preserved from damaging radiation by the steep gradient of the dose distribution away from the source.

The recent introduction of next-generation TPSs that allow image-guided brachytherapy has resulted in an increase in the complexity of the dose distribution [1–3]. However, it can be difficult to evaluate the complicated dose distribution delivered by image-guided brachytherapy by using conventional means, such as film, a thermoluminescence dosimeter or an ion chamber, which are limited to a point or to two dimensions. HDR brachytherapy dosimetry tools with a higher spatial resolution are required.

Polymer gel dosimeters are expected to serve as three-dimensional (3D) dosimeters [4–6]. In polymer gel dosimeters, the radiation induces polymerisation of the monomers in the gel matrix, thereby recording the radiation dose distribution in three dimensions. Dose data from polymer gel dosimeters can be measured using imaging techniques. Magnetic resonance imaging (MRI), optical CT and X-ray CT are commonly used techniques [4]. Within a certain dose range, the amount of polymerisation is directly proportional to the spin–spin relaxation rate (R_2) of the hydrogen nucleus; this means that the absorbed dose fixated in the polymer gel can be measured using MRI. Approaches to using polymer gel dosimeters for HDR brachytherapy have been studied for more than 20 years. In 1996, the dose distribution around a radiation source using BANG gel was measured in a study by Maryanski et al.; they reported a good agreement between the evaluated dose distribution and the TPS calculations for a Ir-192 source in single dwell position [7]. In 1999, the effectiveness for single source dwell position using

* Corresponding author at: School of Allied Health Sciences, Kitasato University, Kanagawa 252-0373, Japan.
E-mail address: y-nabe@kitasato-u.ac.jp (Y. Watanabe).

https://doi.org/10.1016/j.ejmp.2018.12.007
Received 27 September 2018; Received in revised form 21 November 2018; Accepted 10 December 2018
Available online 26 December 2018

polyacrylamide gel was demonstrated by McJury et al. [8]. Hurley at al. reported the use of a high-resolution 4.7 T micro-imaging MR spectrometer for the verification of dose distribution using gel dosimetry for HDR brachytherapy [9]. In the simulation of a real, clinical HDR brachytherapy case, involving multiple catheters and/or source dwell positions, for example, the verification of absolute dose distributions for a clinical treatment plan of intravascular irradiation using *N*-vinylpyrrolidone argon (VIPAR)-based polymer gel was demonstrated in a study of Papagiannis et al. [10]. Kipouros et al. used VIPAR polymer gel to measure the relative dose distribution delivered by an HDR brachytherapy treatment plan for prostate cancer [11]. They reported good agreement between the dose distribution of the target area, which was in the high-dose range, and the TPS calculation for a treatment plan that delivered 20 Gy to the planning target volume (PTV); however, there was a large deviation in the dose distribution of less than 50%. The delivered dose per fraction in HDR brachytherapy for prostate cancer is generally 4–15 Gy, which is higher than that for typical external radiation therapy [3]. When HDR brachytherapy is actually applied, it is important to measure the dose distribution in low-dose regions (such as the locations of organ at risk) in addition to the high-dose range near the source.

In recent years, Hayashi et al. have reported a remarkable increase in the sensitivity of polymer gel dosimeters used with 6 and 10 MV photon beams by adding an inorganic salt ($MgCl_2$) [12–14]. The sensitivity of the gel dosimeter can be adjusted by changing the amount of inorganic salt added. Ono et al. have demonstrated the potential of using a PAGAT type polymer gel dosimeter containing $MgCl_2$ for 3D clinical dosimetry using a 6 MV photon beam [15–17]. The use of these highly sensitive MRI-based gel dosimeters increases the signal-to-noise ratio (SNR), which ultimately leads to a higher precision. However, the sensitisation effect of adding inorganic salt is not clear for low-energy photons such as those of the gamma rays from an Ir-192 source (average energy of 380 keV) [4,14].

The aim of this study was to investigate the accuracy of a treatment plan designed for prostate cancer in the low-dose range using a normoxic *N*-vinylpyrrolidone-based polymer gel (VIPET gel) dosimeter containing inorganic salt as a sensitizer. The fundamental dose characteristics of the gel, such as its dose sensitivity and the dose rate dependence, for gamma rays emitted from the Ir-192 source were investigated in the present study. In addition, gamma analysis was used to compare the dose distribution obtained from the polymer gel dosimeter simulating HDR prostate brachytherapy with that from TPS calculations. We evaluated the measurement accuracy using the sensitised polymer gel dosimeter in the low-dose range under clinical conditions, demonstrating the usefulness of the dosimeter compared with dosimeters with conventional sensitivity.

2. Materials and methods

2.1. Gel preparation

This study used the normoxic VIPET gel proposed by Papadakis et al. and Papoutsaki et al. [18,19]. The VIPET gels were prepared using 4% w/w of monomer *N*-vinylpyrrolidone (NVP, Wako Pure Chemicals, Japan), 4% w/w of cross-linker *N*,*N*′-methylenebisacrylamide (Bis, Wako Pure Chemicals, Japan), 7% w/w of type-A gelatin from porcine skin (G2500, Sigma-Aldrich, UK), 5 mM tetrakis(hydroxymethyl)phosphonium chloride (THPC, 80% in water; Tokyo Kasei Kogyo Co., Ltd., Japan) and 85% w/w of ultra-pure water (Purelab Flex UV, Elga LabWater, UK). "% w/w" refers to mass fraction, and "mM" refers to the molar concentration examined. We also prepared highly sensitive VIPET polymer gel by adding 0.4 M of magnesium chloride ($MgCl_2$) (according the naming of Ono et al. [16,17], hereinafter referred to as iVIPET). For the evaluation of the dose response, glass vials (height, 120 mm; diameter, 40 mm) were filled with the gels. The remaining gel was used to fill a cylindrical glass vessel (height, 125 mm; diameter, 120 mm) for the dose distribution measurement of a clinical treatment plan that simulated HDR prostate brachytherapy. Since the dose responses of polymer gel dosimeters depend on environmental conditions, especially the temperature during preparation and storage [4], all polymer gels were prepared in the same batch. In addition, all the gel dosimeters were stored in a dark room at the same room temperature as the treatment room (23 °C) until irradiation to achieve adequate deoxidising effect by THPC.

2.2. Irradiation of the polymer gels

Immediately before irradiation, a polyacetal flexible catheter (ProGuide Sharp Needle; Elekta, Sweden; length, 200 or 240 mm; diameter, 2 mm) was inserted into the gel dosimeter to transport the Ir-192 source into it. The same remote afterloading system (microSelectron HDR V3; Elekta, Sweden) was used for all the measurements. In this device, the Ir-192 source was a 0.6 mm (diameter) × 3.5 mm (length) iridium pellet in a stainless steel capsule that is welded to a stainless steel cable. The source is guided to the planned source positions and dwell times by a motor-driven system. The air kerma strength of the Ir-192 source for the VIPET and iVIPET tests was 23.127 and 28.751 mGy m^2 h^{-1}, respectively. To evaluate the sensitivity and dose rate dependence, a single catheter was inserted into the centre of the gel dosimeter. The source was held stationary at one position, and the doses of 5, 10, 20, 30, 40, 50, 60, 80 and 100 Gy were delivered to each sample at a radius of 10 mm around the centre of the source (Fig. 1a). The glass vial was also placed in a water-equivalent phantom (Solid Water Phantom; Gammex, USA; dimensions, 40 × 40 × 25 cm) to satisfy the backscattering condition (Fig. 1b).

The dose distribution of a simulated clinical treatment plan was measured with the VIPET and iVIPET gel dosimeters. A custom-made acrylic template was used to attach 18 catheters to the gel dosimeter (Fig. 2a, b). The source was positioned at nine points along the catheters at 5 mm intervals, covering a depth of 40 mm (Fig. 2c). The dwell times for the VIPET and iVIPET trials were 4.8 and 2.8 s, respectively, for all the source positions. The treatment plan delivered an absorbed

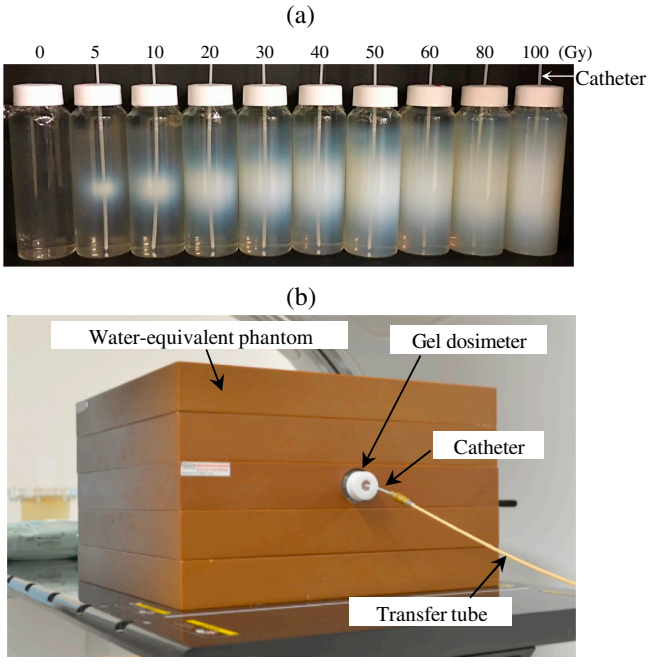

Fig. 1. (a) iVIPET gel dosimeters irradiated at doses of 0–100 Gy. All were irradiated from a single source with the vial positioned 10 mm from the source's transverse bisector. (b) The glass vial was placed in a water-equivalent phantom (dimensions 40 × 40 × 25 cm).

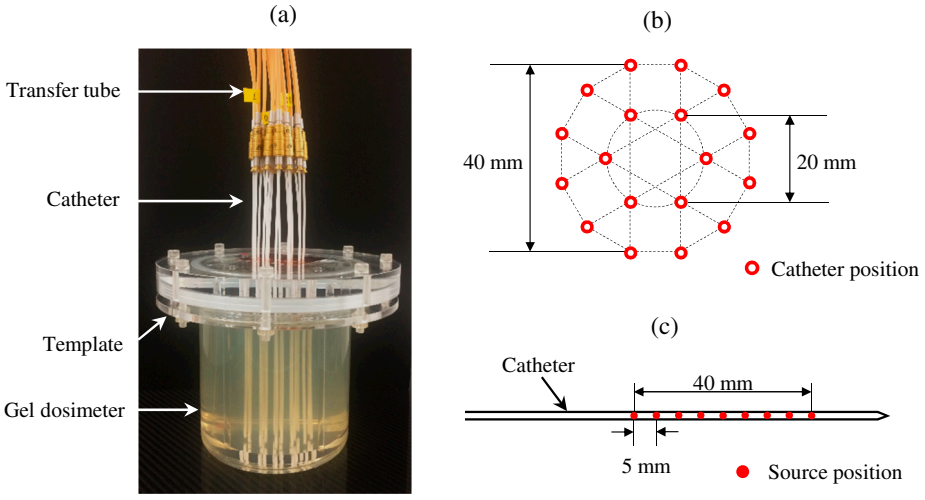

Fig. 2. (a) The iVIPET gel dosimeter used to simulate high-dose-rate prostate brachytherapy. (b) Schematic layout of the 18 flexible catheters (red circles). (c) The sources (red points) were placed at nine points across 40 mm, separated by 5 mm intervals. (For interpretation of the references to colour in this figure legend, the reader is referred to the web version of this article.)

dose of 10 Gy to the PTV; this was designed to reflect the source transport conditions typically used in a clinical context.

2.3. MRI measurements and dose calibrations

After irradiation, the gel dosimeters were stored in the MRI scanner room, and MR images were acquired 24 h after completing the radiation reaction. For the scans, 1.4 mm diameter edible dried pasta was inserted into the catheter to suppress susceptibility artefacts because MRI measurements of the response in gel dosimeters can be affected by distortions in the magnetic field caused by the difference in the magnetic susceptibilities of the gel and catheter. The scans were acquired with a 1.5 T MRI scanner (SIGNA HDxt, GE, USA) with a quadrature head coil, applying a spin echo sequence with the following parameters: repetition time, 4000 ms; echo times (TE), 10 and 250 ms; field of view, 256 mm × 256 mm; and matrix size, 256 × 256. The transverse relaxation time (T_2) map was calculated for each slice using ImageJ v1.47 software. R_2 was determined as

$$R_2 = \frac{1}{T_2} = \frac{1}{TE_2 - TE_1} ln\left(\frac{S_1}{S_2}\right) \quad (1)$$

where S_1 and S_2 are the single intensities at TE_1 and TE_2, respectively. The relationships between absorbed dose and R_2 were obtained using transverse images with 2 mm slices taken according to the source positions. The value of R_2 was calculated for 36 values measured at a radial average of every 10 degrees at a 10-mm distance from the centre of the source. The dose response data were then fitted with the following linear equation:

$$R_2 = gD + R_0 \quad (2)$$

where D is the absorbed dose, and the coefficients of g and R_0 represent the dose sensitivity and the offset of the dose response curve, respectively. The value of R_2 measured after irradiation was converted into the absorbed dose as follows:

$$D = \alpha R_2 + D_0 \quad (3)$$

where α is a conversion factor and D_0 is the offset of the absorbed dose. The dose uncertainty of the gel dosimeter measurements depends on the uncertainty in the dose calibration data and the uncertainty in the R_2 calculation. The relative dose uncertainty of a pixel in the R_2 map with a value of $R_2 \pm \sigma_{R_2}$ can be calculated as follows [20]:

$$\frac{\sigma_D}{D} = \sqrt{\left(\frac{R_2\sigma_\alpha}{D}\right)^2 + \left(\frac{\alpha\sigma_{R_2}}{D}\right)^2 + \left(\frac{\sigma_{D_0}}{D}\right)^2} \quad (4)$$

where σ_α and σ_{D_0} are the standard deviations of α and D_0, respectively. The dose resolution of the gel dosimeter, D_Δ^p, is related to the dose uncertainty σ_D as follows [21]:

$$D_\Delta^p = k_p \bullet \sqrt{2} \bullet \sigma_D \quad (5)$$

where k_p is the coverage factor for the confidence interval p. For the 95% confidence level, k_p is 1.96. The relative dose uncertainty σ_D/D and dose resolution $D_\Delta^{95\%}$ of the VIPET and iVIPET gels were compared within their linear response regions.

2.4. Dose rate dependence

The dose rate varies with the distance from the centre of the source. The dose rate dependence was evaluated by investigating the dose sensitivity corresponding to the distance from the centre of the source for each vial of different doses (dwell time at single source position). The dose rate and absorbed dose were calculated by TPS [2]. The value of R_2 was calculated for 36 values measured at a radial average of every 10 degrees for each distance from the centre of the source. The ranges for the dose rates measured by the VIPET and iVIPET gel dosimeters were 1.5–25.4 and 1.9–31.5 Gy min^{-1}, respectively. These ranges corresponded to positions 4–17 mm from the centre of the source, and R_2 was measured in steps of 1 mm.

2.5. Verification of the simulated clinical plan dose distribution

Dose distributions were measured from transverse images (5 mm slices) of the prostate cancer clinical plan at the centre of the source dwell region. The value of R_2 measured after irradiation was converted into the absorbed dose using the dose–R_2 response curves shown in Fig. 3. The R_2 homogeneity was evaluated by the use of the gel phantom before irradiation [22]. These dose distributions were then compared with those calculated by the TPS using gamma analysis with a 2%/2 mm criterion along with the gamma index analysis software Simple IMRT Analysis (Triangle Products, Japan) [23]. The dose profile at the centre and the 2% dose difference were also evaluated for each dose range. The 2% dose difference for iVIPET and VIPET was evaluated with the same size of the field of view (85 × 85 mm).

The TPS (Oncentra; Elekta, Sweden) calculated the dose according to the American Association of Physicists in Medicine protocol in publication TG-43 [24] with a grid size of 1 mm. After performing MR imaging for obtaining dose data, the gel dosimeter was imaged with computed tomography (CT) for dose distribution calculations by the TPS because it avoids the effect of the dose from CT scan. The

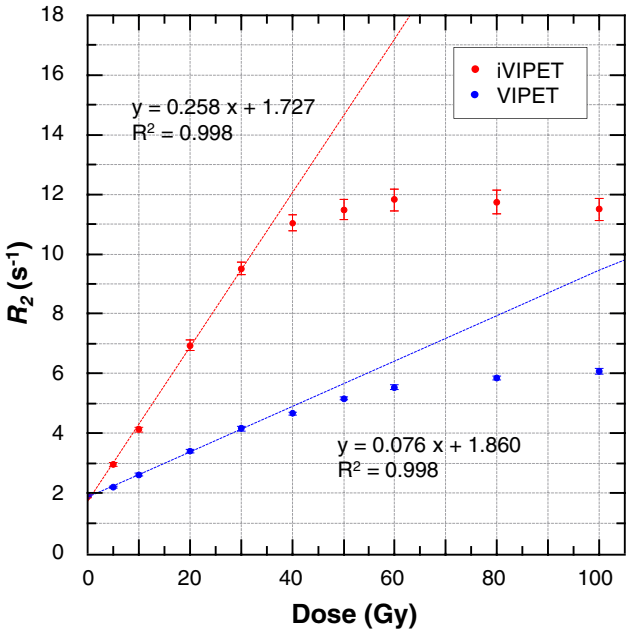

Fig. 3. Dose–relaxation rate (R_2) response curves for the iVIPET and VIPET gel dosimeters. The dashed lines represent linear fits to the data in the dose range 0–30 Gy.

geometrical positions of the CT and MR images were matched using a 5 mm diameter acrylic rod placed orthogonally within the dosimeter.

3. Results

3.1. Dose–R_2 response

The dose–R_2 response curves of the VIPET and iVIPET gel dosimeters are shown in Fig. 3. At doses of up to 30 Gy, the sensitivity of iVIPET ($0.258 \pm 0.002\,s^{-1}\,Gy^{-1}$) in the linear response region was 3.4 times higher than that of VIPET ($0.076 \pm 0.001\,s^{-1}\,Gy^{-1}$). The calculated uncertainties and dose resolutions of the measured doses at the 95% confidence level are plotted in Fig. 4 as functions of the delivered dose. The dose uncertainties for the VIPET and iVIPET gels were 7.8% and 3.3% at 5 Gy, respectively, and 1.8% and 1.0% at 30 Gy (Fig. 4a). At lower doses, the dose uncertainty for iVIPET was particularly small relative to that of VIPET. At doses of up to 30 Gy, the dose resolution at the 95% confidence level for iVIPET was < 1 Gy (Fig. 4b). Values of $\alpha \pm \sigma_\alpha$ for VIPET and iVIPET were 13.010 ± 0.105 and 3.856 ± 0.025, respectively, and values of σ_{D_0} were 0.312 and 0.146, respectively. Fig. 5 shows the dose sensitivities of VIPET and iVIPET at dose rates corresponding to 4–17 mm from the centre of the source. The coefficient of variation at iVIPET was 6% and that at VIPET was 3%.

3.2. Verification of the simulated clinical plan dose distribution

The R_2 homogeneity evaluated by gel dosimeter before irradiation was 88% in the field of view for the dose distribution verification. Fig. 6 shows the T_2 maps with and without edible dried pasta inside the catheter in the preliminary experiments. The effect of suppressing susceptibility artifacts by edible dried pasta was confirmed. The dose distributions measured by the iVIPET and VIPET gel dosimeters in the transverse plane at the centre of the source dwelling area are shown in Fig. 7a, along with the TPS calculations. The gamma passing rates of the iVIPET and VIPET gels according to the 2%/2 mm criterion were 97.9% and 90.1%, respectively (Fig. 7b). The uncertainty within 3 mm from

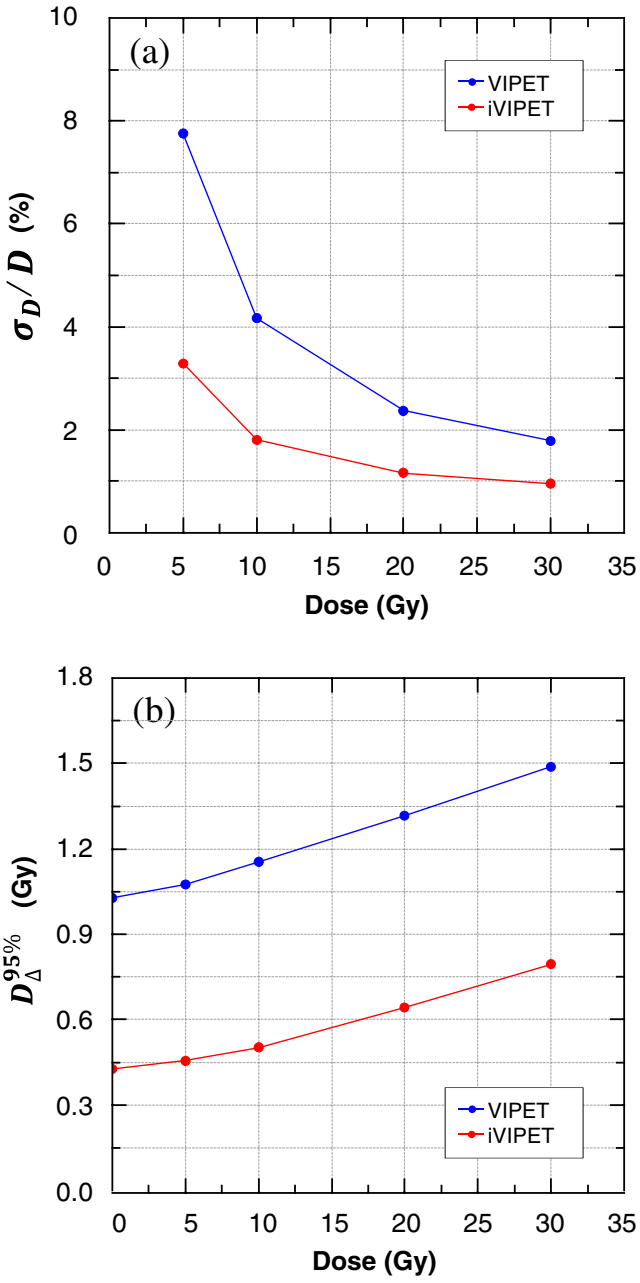

Fig. 4. (a) Dose uncertainties of the iVIPET and VIPET dosimeters in the linear response region. (b) The dose resolution at the 95% confidence level.

the centre of the source was relatively large for the iVIPET gel. The iVIPET results were in good agreement with the TPS calculations, but the VIPET dosimeters were superior in measurement of the dose distribution near the catheter. The dose profile of the VIPET gel was noisier than that of the iVIPET gel (Fig. 8). The minimum dose within the field of view for evaluation of 2% difference between iVIPET and VIPET was 1.2 Gy. The proportions of pixels that satisfied the 2% dose difference in the dose range 1.2–10 Gy were 99.6% and 88.5% for the iVIPET and VIPET gels, respectively (Fig. 9). This dose range corresponds to locations outside the PTV.

4. Discussion

The findings of this study confirmed that the sensitivity of iVIPET

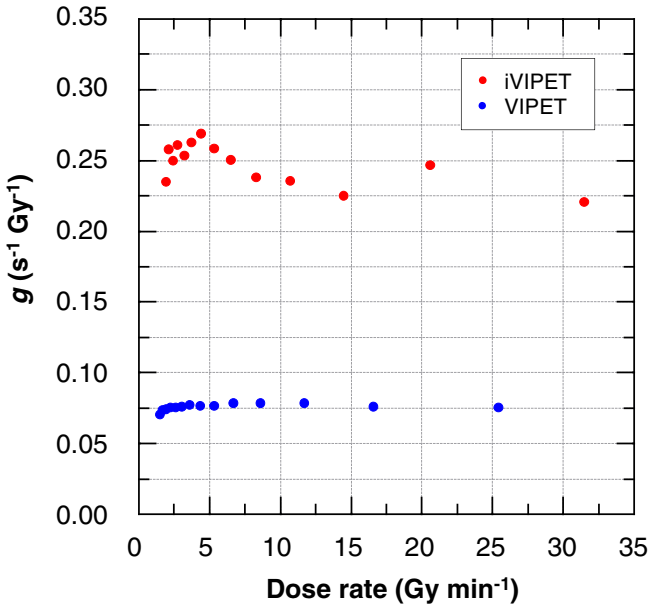

Fig. 5. Dose sensitivity (g) of the iVIPET and VIPET gel dosimeters as a function of dose rate.

gel to low-energy gamma rays emitted from an Ir-192 source was 3.4 times higher than that of VIPET gel. This was consistent with the results of Hayashi et al. [14]. In the past, attempts to improve the sensitivity of VIP-based polymer gels have included using another gelling agent [25] or increasing the amount of the monomer [26]; however, adding inorganic salt is the most effective approach. In the iVIPET and VIPET gel dosimeters, dose rate dependence was not observed in the range of 1.5–25.4 and 1.9–31.5 Gy min^{-1}, respectively, as compared with the MAG-type in which dose rate dependence has been reported [27,28]. Consistent with the results of this study, Hayashi et al. concluded that the dose sensitivity of VIPET gel dosimeters containing $MgCl_2$ does not depend on the dose rate in 1.0, 2.0, 3.0 and 5.0 Gy min^{-1} dose rates for 10 MV photon beams [14]. However, all points in the dose distribution for the clinical treatment plan will have a significant range of dose rate histories as the dose at each point will have contributions from different Ir-192 sources. This may lead to a possibility of uncertainty in dose distribution verification using iVIPET and VIPET dosimeters as the evaluation of the dose rate dependence in this study was limited to an area of ≤17 mm from the centre of the source.

In the present study, the increased sensitivity provided by the iVIPET gel dosimeter improved uncertainty and dose resolution. The dose resolution at 95% confidence level of iVIPET did not achieve 2% of the clinical dose, which is the dose precision recommended by the International Commission on Radiation Units and Measurements (Report No. 42) for the dose verification of the treatment plan [29]. We decided the echo time with reference to the pulse sequence adopted by Hayashi et al [14]. This study unified the pulse sequence for iVIPET and VIPET gel. The uncertainty pertaining to the R_2 values and the dose resolution is determined by the choice of the echo time. In addition, TE optimization and multi-spin-echo sequence are recommended for polymer gel dosimetry [30,31]. Although single-spin-echo was used in this study, dose resolution can be significantly improved with the use of multi-spin-echo sequence and by the optimal selection of echo time. Further, the measurement of the R_2 distribution in a homogeneous phantom and the use of this image-set as a template to correct the resulting R_2 images may have been effective; however, this was not used in this study [32].

MR images with a fine spatial resolution are indispensable for measuring the steep-gradient dose distributions applied in HDR brachytherapy. Several factors may contribute to the dose uncertainty of MR-based polymer gel dosimetry. Vandecasteele et al. and De Deene et al. attributed the dose uncertainty in polymer gel dosimeters to several factors such as the stochastic noise, calibration uncertainties, temperature drift, and R_2 image non-uniformities [33–37]. Increasing the sensitivity of the gel dosimeter improves the SNR of the R_2 map in the low-dose range. Ensuring a sufficient SNR in a high-resolution MR image requires a long scan time, but this should be shortened by using a highly sensitive polymer gel in the dosimeter.

The dose distributions of the prostate cancer clinical plan measured by the iVIPET gels were in good agreement with those calculated by the TPS. In particular, the iVIPET gel proved useful for low doses in the clinical plan, which tended to be measured inaccurately with the VIPET gel. Thus, low doses are amenable to more accurate measurements with the iVIPET gel than with the VIPET gel. When HDR brachytherapy is actually used, the dose constraints for organs at risk must be considered to prevent severe radiation damage. Dosimeters must therefore be able to detect the unexpected hotspots as well as the unexpected low-dose regions. In this study, the dose distributions with treatment plans that delivered 10 Gy to the PTV were measured using catheters positioned at relatively wide intervals. This treatment plan delivered a much smaller dose than that of Kipouros et al. [11]; in addition, our results verified the dose distribution at the low-dose range (< 10 Gy). The iVIPET dosimeter has been shown to exhibit a linear response to doses in the range 0–30 Gy, a range that covers the doses typically delivered in HDR

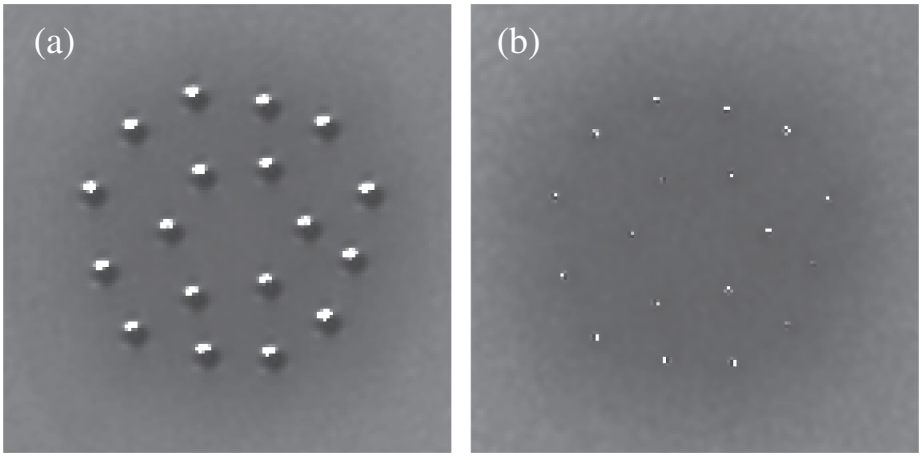

Fig. 6. The effect of suppressing susceptibility artifacts on T_2 map by edible dried pasta inside the catheter. T_2 maps (a) without pasta and (b) with pasta are shown.

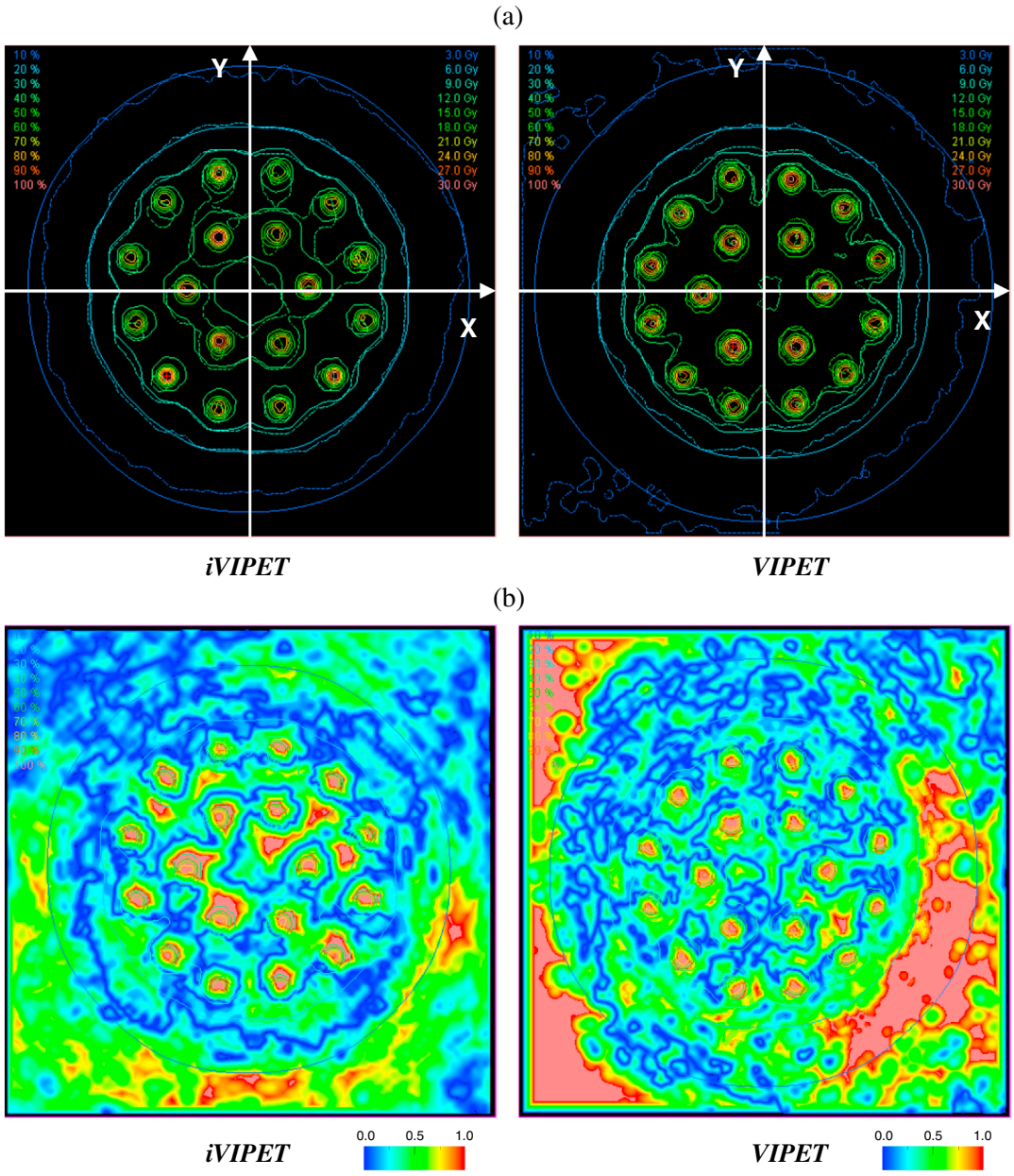

Fig. 7. Comparison of the dose distributions in the transverse plane at the centre of the source dwelling area between the two gel dosimeters and the treatment planning system calculations. (a) Percentages of the isodose contours for the iVIPET and VIPET gel dosimeters (dotted lines) and the calculations returned by the treatment planning system (solid lines). (b) Results of gamma analysis with the 2%/2 mm criterion.

brachytherapy for treatment of prostate cancer.

There was some uncertainty in the conditions around the Ir-192 source. We used polyacetal flexible catheters to transport the Ir-192 source. De Deene et al. have reported further specific dosimetric uncertainties pertaining to HDR brachytherapy [38]. They provided an overview of several causes of uncertainty in 3D dose verification of brachytherapy, which included the oxygen permeability of the catheter material, diffusion of monomers during radiation, partial volume effects, magnetic susceptibility effects, and saturation. We will further investigate the characteristics of polymer gel dosimeter for HDR brachytherapy in the future. Dose distribution comparison methods such as gamma analysis may underestimate the uncertainty [39]. In this study, the gel responses and TPS calculations were compared in detail by evaluating the dose difference of the calculated dose within each dose range (Fig. 9). This showed that measurement accuracy in the low-dose range improved with the high sensitivity provided by the iVIPET gel.

5. Conclusions

The iVIPET gel dosimeter used in this study was shown to be 3.4 times more sensitive than the VIPET gel dosimeter for the low-energy photons from the Ir-192 source. Thus, iVIPET gel dosimeters can be used to accurately measure the dose distribution of a simulated HDR brachytherapy treatment plan for prostate cancer, even with significant uncertainty directly adjacent to the source. Increasing the sensitivity of the dosimeter gel improved the SNR in the R_2 map and the accuracy of dose conversion. The dose resolution can be improved by optimizing the echo times and using a multi-spin-echo sequence instead of a single-spin-echo sequence. We conclude that the iVIPET gel dosimeter could be a useful tool for verifying the dose distributions of TPS calculations in clinical cases. In future studies, we are planning to optimise the sensitivity of the gel and to combine gels of different sensitivities to enable various dose ranges to be measured most effectively.

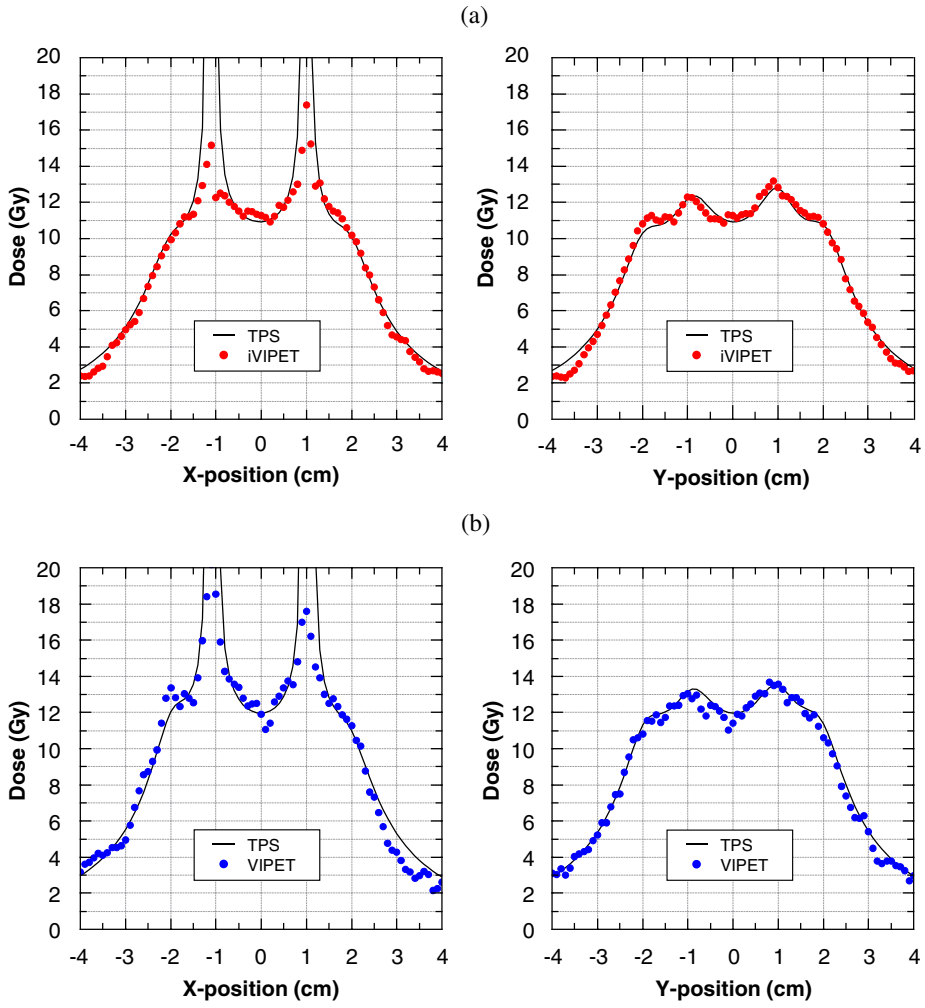

Fig. 8. Comparison of dose distributions in the transverse plane at the centre of the source dwelling area. Dose profiles measured along the *X*- and *Y*-axes with (a) iVIPET gel dosimeters and (b) VIPET gel dosimeters.

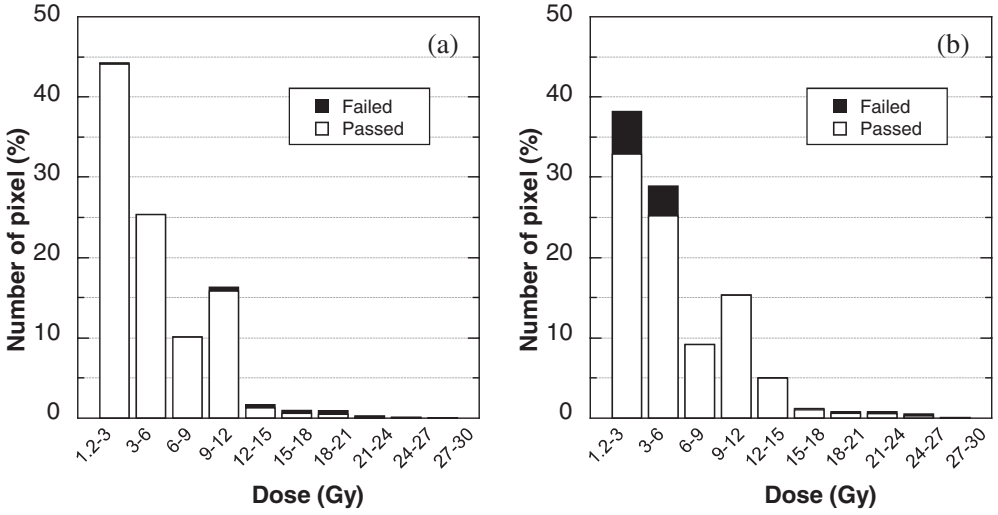

Fig. 9. Performance in the assessment of 2% dose difference in the transverse plane at the centre of the source dwelling area for (a) iVIPET gel and (b) VIPET gel.

Acknowledgements

Funding: This work was supported by JSPS KAKENHI [grant number JP18K07769]; and Kitasato University School of Allied Health Science [Grant-in Aid for Research Project number 2018-1047].

Appendix A. Supplementary data

Supplementary data to this article can be found online at https://doi.org/10.1016/j.ejmp.2018.12.007.

References

[1] Hellebust TP, Kirisits C, Berger D, Pérez-Calatayud J, De Brabandere M, De Leeuw A, et al. Recommendations from Gynaecological (GYN) GEC-ESTRO Working Group: considerations and pitfalls in commissioning and applicator reconstruction in 3D image-based treatment planning of cervix cancer brachytherapy. Radiother Oncol 2010;96:153–60.

[2] Kirisits C, Rivard MJ, Baltas D, Ballester F, De Brabandere M, van der Laarse R, et al. Review of clinical brachytherapy uncertainties: analysis guidelines of GEC-ESTRO and the AAPM. Radiother Oncol 2014;110:199–212.

[3] Hoskin PJ, Colombo A, Henry A, Niehoff P, Hellebust TP, Siebert FA, et al. GEC/ESTRO recommendations on high dose rate afterloading brachytherapy for localised prostate cancer: an update. Radiother Oncol 2013;107:325–32.

[4] Baldock C, De Deene Y, Doran S, Ibbott G, Jirasek A, Lepage M, et al. Polymer gel dosimetry. Phys Med Biol 2010;55:R1–63.

[5] Rabaeh KA, Basfar AA, Almousa AA, Devic S, Moftah B. New normoxic N-(Hydroxymethyl)acrylamide based polymer gel for 3D dosimetry in radiation therapy. Phys Med 2017;33:121–6.

[6] Abtahi SM, Pourghanbari M. A new less toxic polymer gel dosimeter: radiological characteristics and dosimetry properties. Phys Med 2018;53:137–44.

[7] Maryanski MJ, Ibbott GS, Eastman P, Schulz RJ, Gore JC. Radiation therapy dosimetry using magnetic resonance imaging of polymer gels. Med Phys 1996;23:699–705.

[8] McJury M, Tapper PD, Cosgrove VP, Murphy PS, Griffin S, Leach MO, et al. Experimental 3D dosimetry around a high-dose-rate clinical ^{192}Ir source using a polyacrylamide gel (PAG) dosimeter. Phys Med Biol 1999;44:2431–44.

[9] Hurley C, McLucas C, Pedrazzini G, Baldock C. High-resolution gel dosimetry of a HDR brachytherapy source using normoxic polymer gel dosimeters: preliminary study. Nucl Instrum Methods Phys Res 2006;565:801–11.

[10] Papagiannis P, Pappas E, Kipouros P, Angelopoulos A, Sakelliou L, Baras P, et al. Dosimetry close to an ^{192}Ir HDR source using *N*-vinylpyrrolidone based polymer gels and magnetic resonance imaging. Med Phys 2001;28:1416–26.

[11] Kipouros P, Papagiannis P, Sakelliou L, Karaiskos P, Sandilos P, Baras P, et al. 3D dose verification in ^{192}Ir HDR prostate monotherapy using polymer gels and MRI. Med Phys 2003;30:2031–9.

[12] Hayashi S, Fujiwara F, Usui S, Tominaga T. Effect of inorganic salt on the dose sensitivity of polymer gel dosimeter. Radiat Phys Chem 2012;81:884–8.

[13] Hayashi S, Kawamura H, Usui S, Tominaga T. Comparison of the influence of inorganic salts on the NMR dose sensitivity of polyacrylamide-based gel dosimeter. J Phys Conf Ser 2013;444:012094.

[14] Hayashi S, Kawamura H, Usui S, Tominaga T. Influence of magnesium chloride on the dose–response of polyacrylamide-type gel dosimeters. Radiol Phys Technol 2018;11:375–81.

[15] Ono K, Fujimoto S, Hayashi S, Miyazawa M, Akagi Y, Hirokawa Y. Development of 3D dose verification system for volumetric modulated arc therapy using improved polyacrylamide-based gel dosimeter. Med Phys 2014;41:246.

[16] Ono K, Fujimoto S, Hayashi S, Miyazawa M, Akagi Y, Hirokawa Y. Dosimetric evaluation of ArcCHECK and 3DVH system using customized polymer gel dosimeter. Med Phys 2015;42:3406.

[17] Ono K, Fujimoto S, Hayashi S, Hioki K, Miyazawa M, Akagi Y, et al. Dosimetric evaluation of the respiratory interplay effect during VMAT delivery using IPAGAT polymer gel dosimeter. Med Phys 2016;43:3634.

[18] Papadakis AE, Maris TG, Zacharopoulou F, Pappas E, Zacharakis G, Damilakis J. An evaluation of the dosimetric performance characteristics of *N*-vinylpyrrolidone-based polymer gels. Phys Med Biol 2007;52:5069–83.

[19] Papoutsaki MV, Maris TG, Pappas E, Papadakis AE, Damilakis J. Dosimetric characteristics of a new polymer gel and their dependence on post-preparation and post-irradiation time: effect on X-ray beam profile measurements. Phys Med 2013;29:453–60.

[20] Baldock C, Murry P, Kron T. Uncertainty analysis in polymer gel dosimetry. Phys Med Biol 1999;44:N243–6.

[21] Baldock C, Lepage M, Back SAJ, Murry PJ, Jayasekera PM, Porter D, et al. Dose resolution in radiotherapy polymer gel dosimetry: effect of echo spacing in MRI pulse sequence. Phys Med Biol 2001;46:449–60.

[22] National Electrical Manufacturers Association. Determination of image uniformity in diagnostic magnetic resonance images. NEMA Standards Publication MS 3-2008, 2008;1–17.

[23] Low DA, Dempsey JF. Evaluation of the gamma dose distribution comparison method. Med Phys 2003;30:2455–64.

[24] Rivard MJ, Coursey BM, DeWerd LA, Hanson WF, Huq MS, Ibbott GS, et al. Update of AAPM Task Group No. 43 Report: a revised AAPM protocol for brachytherapy dose calculations. Med Phys 2004;31:633–74.

[25] Maeyama T, Ishida Y, Kudo Y, Fukasaku K, Ishikawa K, Fukunishi N. Polymer gel dosimeter with AQUAJOINT® as hydrogel matrix. Radiat Phys Chem 2018;146:121–5.

[26] Kozicki M, Jaszczak M, Maras P, Dudek M, Cłapa M. On the development of a VIPARnd radiotherapy 3D polymer gel dosimeter. Phys Med Biol 2017;62:986–1008.

[27] De Deene Y, Vergote K, Claeys C, De Wagter C. The fundamental radiation properties of normoxic polymer gel dosimeters: a comparison between a methacrylic acid based gel and acrylamide based gels. Phys Med Biol 2006;51:653–73.

[28] Karlsson A, Gustavsson H, Månsson S, McAuley KB, Bäck SÅJ. Dose integration characteristics in normoxic polymer gel dosimetry investigated using sequential beam irradiation. Phys Med Biol 2007;52:4697–706.

[29] ICRU. Use of computers in external beam radiotherapy procedures with high-energy photons and electrons. 1987. Report No 42.

[30] De Deene Y, Van de Walle R, Achten E, De Wagter C. Mathematical analysis and experimental investigation of noise in quantitative magnetic resonance imaging applied in polymer gel dosimetry. Signal Process 1998;70:85–101.

[31] De Deene Y, Baldock C. Optimization of multiple spin-echo sequences for 3D polymer gel dosimetry. Phys Med Biol 2002;47:3117–41.

[32] De Deene Y. Fundamentals of MRI measurements for gel dosimetry. J Phys: Conf Ser 2004;3:87–114.

[33] Vandecasteele J, De Deene Y. On the validity of 3D polymer gel dosimetry: I. reproducibility study. Phys Med Biol 2013;58:19–42.

[34] Vandecasteele J, De Deene Y. On the validity of 3D polymer gel dosimetry: II. physico-chemical effects. Phys Med Biol 2013;58:43–61.

[35] Vandecasteele J, De Deene Y. On the validity of 3D polymer gel dosimetry: III. MRI-related error sources. Phys Med Biol 2013;58:63–85.

[36] De Deene Y, Vandecasteele J. On the reliability of 3D gel dosimetry. J Phys: Conf Ser 2013;444:012015.

[37] Kipouros P, Pappas E, Baras P, Hatzipanayoti D, Karaiskos P, Sakelliou L, et al. Wide dynamic dose range of VIPAR polymer gel dosimetry. Phys Med Biol 2001;46:2143–59.

[38] De Deene Y, Reynaert N, De Wagter C. On the accuracy of monomer/polymer gel dosimetry in the proximity of a high-dose-rate ^{192}Ir source. Phys Med Biol 2001;46:2801–25.

[39] Senkesen O, Tezcanli E, Buyuksarac B, Ozbay I. Comparison of 3D dose distributions for HDR ^{192}Ir brachytherapy sources with normoxic polymer gel dosimetry and treatment planning system. Med Dosim 2014;39:266–71.